VOL. 12, NO. 16, AUGUST 2017 ISSN 1819-6608
ARPN Journal of Engineering and Applied Sciences

www.arpnjournals.com

RENEWABLE ENERGY SYSTEMS WITH INTEGRATED ACTIVE FILTER CAPABILITIES

Pathan Soheba Taj, J Jayachandran and Malathi S
Department of Electrical and Electronics Engineering, AP-III SASTRA University, India
E-Mail: pathansoheba@gmail.com

ABSTRACT

Conventional energy sources are not preferred, rather, wind energy is mainly used which is a renewable source of energy and is unlimited in nature. Wind turbines are of two types-variable speed wind turbine and fixed speed wind turbine. At distinct wind speeds, wind turbine has to run at variable rotor speed to obtain the maximum power. Power converters can be used to accomplish the maximum power. DFIG is one among variable speed wind turbine and is mainly considered, due to its high energy output, damping performance, low- converter rating and low cost. Another renewable source of energy which is nothing but solar energy is incorporated by applying Synchronous reference frame algorithm. For improving power quality and to obtain maximum power wind energy conversion system (WECS) is provided with doubly fed induction generator (DFIG). The role of rotor side converter (RSC) is to distribute reactive power to DFIG whereas grid side converter (GSC) is used to get even DC voltage and reduce harmonics which is due to non-linear load. WECS acts like DFIG to reduce deviations and distortions of voltage and current from sinusoidal waveform even when the wind turbine is at halt. In case of solar system, for reactive power compensation and to get three phase active power the SPV system is linked to VSC. For extracting maximum power and to increase the efficiency from the SPV array, a single-stage three phase grid system is used along MPPT technique which is integrated with the synchronous reference frame algorithm. Both the sources are compared and the best system out of the two systems has been obtained using MATLAB simulation.

Keywords: DFIG, WECS, rotor side converter, grid side converter, SPV, voltage source converter.

1. INTRODUCTION

Wind energy is fast emerging renewable energy source. Wind energy and solar energy are mainly taken into consideration because of its abundance and eco-friendly nature. Conventional sources causes harm to environment and are high in cost hence it is not preferred mainly.

Wind turbines are of two types-variable and fixed speed wind turbines. DFIG which is a variable speed wind turbine is mainly preferred along with induction generator or PMSG. In this project induction generator is used and is coupled with the wind turbine. Out of the two wind turbines, variable speed wind turbines gives better energy capturing capability. For weak grid, the DFIG used here gives good damping performance. Due to its high energy output, damping performance, low converter rating and lower cost DFIG is mainly preferred.

For mitigating harmonics which are produced due to nonlinear load, a control algorithm for GSC is used. Though the wind turbine is in staling condition, the DFIG works like an active filter which is an advantage. For controlling grid side converter Hysteresis controller is used whereas rotor side converter is controlled using PWM generator. MPPT algorithm is used to extract the maximum power and to get the reference wind speed. To extract the reference load currents synchronous reference frame control method is used.

There are various types of MPPT algorithm techniques like Perturb and observe algorithm, Incremental conductance algorithm, Hill climbing algorithm, Fuzzy logic control, Neural network. In this perturb and observe is preferred as it is simple to implement and gives acceptable performance. MPPT (P&O) can be used in two ways, by the selection of control methods such as reference voltage and by duty ratio.

In case of solar energy source, SPV system is mainly used to supply power to remote areas and it is easy to install and require low maintenance. A single stage topology is preferred than conventional double stage topology as it is more effective in reducing the losses. Whereas in double stage topology, first stage is used for extracting maximum power and the second stage is used to send that extracted power to the distribution network.

A SRF-synchronous reference frame algorithm is used along with VSC to extract the fundamental active and reactive components of load current for estimating the three phase sensed supply currents. There are many time domain and frequency domain algorithms used, in which time domain algorithm is implemented. The other algorithms are not preferred as it involves complex blocks and requires huge calculations and equations.

Direct current control and indirect current control are the two techniques used. For eliminating harmonics and to reduce the THD to less than 5% indirect current control technique is preferred.

2. WIND ENERGY CONVERSION SYSTEM

Table-1. Existing system and proposed system differences.

Existing system	Proposed system
In this system, Direct current control is used	In this system, Indirect current control is used

THD cannot be reduced to below 5%	THD value can be reduced below 5%
DFIG is not used here	DFIG acts like an active filter

2.1 STATCOM

STATCOM is a Static Synchronous Compensator which is a regulating device used on AC transmission network. It is a member of FACTS devices. STATCOM acts as source or sink of reactive power and is based on VSC (Voltage Source Converter). WECS-Wind Energy Conversion System works as Static Synchronous Compensator.

Fluctuation in power due to the large penetration of wind influences the power quality. Power quality problems like voltage flicker, frequency deviations significantly. Wind turbines like variable speed turbines are equipped with power electronic devices, which mainly use PWM inverters and IGBT (Insulated Gate Bipolar Transistor) technology. The demerit of PWM technique is that it produces harmonic current.

3. DOUBLY FED INDUCTION GENERATOR (DFIG)

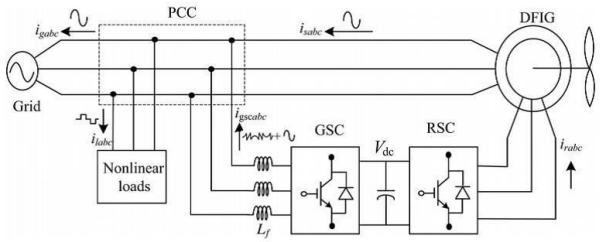

Figure-1. Proposed system configuration.

Wind turbine systems are classified as- Fixed speed and Variable speed wind turbines. To get the maximum power, at different wind conditions machine should run at different rotor speeds, hence Variable speed wind turbines are preferred. There are various variable speed wind turbines out of which DFIG is preferred due to its high energy output, low converter rating.

The system has wound round induction generator and an IGBT based PWM converter. Two converters are used which are RSC and GSC. RSC is connected to the rotor of DFIG whereas stator is connected directly to AC mains. The two converters are connected back-to-back, which are placed between the rotor and the grid. By Voltage oriented reference frame the RSC is used to obtain the maximum power and the GSC is used to mitigate harmonic currents produced by non-linear load. To get the fundamental component of load current SRF (Synchronous Reference Frame) control method is used.

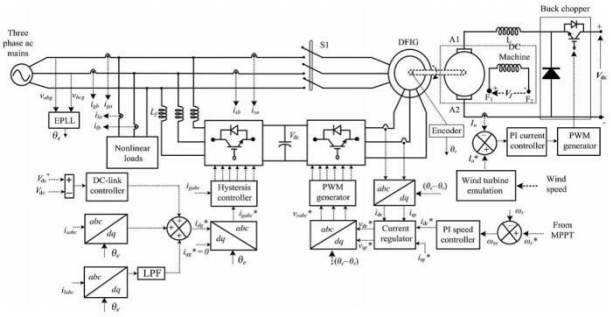

Figure-2. Schematics of control algorithm of WECS.

The two converters are linked using a DC capacitor and is used for the storage of power from the induction generator. The slip power flows in both direction that is from supply to rotor and from rotor to supply. Hence the speed can be controlled by either of the converters in both sub-synchronous and super-synchronous speed. Machine operates in two modes, Motoring mode is below synchronous speed and the generating mode is above synchronous speed. RSC works like a rectifier and GSC works like an inverter. When the motoring mode takes place above synchronous speed and the generating mode is below synchronous speed, RSC works as an inverter and GSC works as a rectifier.

DFIG is connected to the DC machine. By providing duty ratio a fixed value to the chopper the DC machine runs at stable speed and from the grid the stator is kept isolated. For obtaining duty ratio to the chopper current controller plays main role. By maintaining the field voltage to a fixed value, flux of the machine is kept constant. By controlling DC machine, wind turbine mode can be obtained after the conversion from duty ratio mode. Due to the absence of real power flow to the grid from DFIG, the speed controller comes into action by gradually maintaining the DC machine speed to higher or maximum.

4. CONTROL OF GRID SIDE CONVERTER (GSC)

4.1 Hysteresis controller

The simple circuit model of hysteresis controller is shown in Figure-2.1. The switching pulse for the GSC is given from hysteresis current controller. The actual voltage V_{dc} and the desired voltage V_{dc}^{*} are compared and the output is fed to the DC link controller to get the Active power component of GSC current and is given in the equation as

$$i_{gsc}^{*}(K) = i_{gsc}^{*}(K-1) + K_{pdc}\{V_{dce}(K) - V_{dce}(K-1)\} + K_{idc}V_{dce}(K) \quad (1)$$

where,

K_{pdc} and K_{idc} are gains of DC link voltage controller.
$V_{dce}(K)$ and $V_{dce}(K-1)$ are the errors of DC-link voltage at the instants of $(K)th$ and $(K-1)th$

Active power component of GSC currents at $(K)th$ and $(K-1)th$ instants are $i_{gsc}^{*}(K)$ and $i_{gsc}^{*}(K-1)$.

Real component of stator current (i_{ds}) is obtained by the combination of sensed stator current (i_{sabc}) and abc to dq transformation and same is obtained by the equation as

$$i_{ds} = (2/3)[i_{sa}\sin\theta_e + i_{sb}\sin(\theta_e - 2\pi/3) + i_{sc}\sin(\theta_e + 2\pi/3)] \quad (2)$$

DC value of load current in synchronously rotating dq frame (i_{ld}) is obtained by the combination of three phase load current (i_{labc}) and the phase angle from EPLL. Both are fed to the abc to dq transformation and the output obtained is then sent to the PI controller.

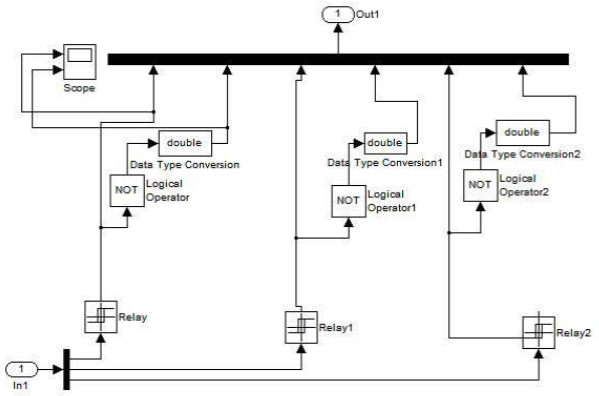

Figure-3. Control of hysteresis controller.

Direct axis component of reference grid current is obtained by using equation

$$i_{dg}^* = i_{gsc}^* + i_{ds} - i_{ld} \quad (3)$$

i_{dg}^* and the EPLL phase angle are fed to the dq to abc transformation to get the reference current i_{gabc}^*. The actual current and the reference current are compared and the obtained output is fed to the hysteresis controller for generating gate pulse to three-phase GSC.

5. ROTOR SIDE CONVERTER (RSC) CONTROL

The direct axis reference rotor current i_{dr}^*can be obtained by comparing the actual speed (ω_r) and the reference speed (ω_r^*). The outputobtained is the error speed and is then sent to the PI speed controller.

$$i_{dr}^*(K) = i_{dr}^*(K-1) + K_{pd}\{\omega_{er}(K) - \omega_{er}(K-1)\} + K_{id}\omega_{er}(K) \quad (4)$$

where,

K_{pd} *and* K_{id} are the constants of PI speed controller. Speed errors at $(K)th$and $(K-1)th$instants are $\omega_{er}(K)$and $\omega_{er}(K-1)$ whereas direct axis reference rotor current at $(K)th$and $(K-1)th$instants are$i_{dr}^*(K)$ *and* $i_{dr}^*(K-1)$.

The actual direct axis rotor current (i_{dr}) and quadrature axis rotor current (i_{qr}), reference direct axis rotor current (i_{dr}^*) and quadrature axis rotor current (i_{qr}^*) are compared. The actual direct and quadrature axis rotor currents are obtained from the reference rotor currents.

$$i_{dr} = (2/3)[i_{ra}\sin\theta_{slip} + i_{rb}\sin(\theta_{slip} - 2\pi/3) + i_{rc}\sin(\theta_{slip} + 2\pi/3)] \quad (5)$$

$$i_{qr} = (2/3)[i_{ra}\sin\theta_{slip} + i_{rb}\sin(\theta_{slip} - 2\pi/3) + i_{rc}\sin(\theta_{slip} + 2\pi/3)] \quad (6)$$

where $\theta_{slip} = \theta_e + \theta_r$

The output is fed to the PI controller to get the reference rotor direct voltage (V_{dr}^*) and reference rotor quadrature voltage (V_{qr}^*)

$$V_{dr}^* = V_{dr}' + (\omega_e - \omega_r)\sigma L_r i_{dr} \quad (7)$$

$$V_{qr}^* = V_{qr}' + (\omega_e - \omega_r)(L_m i_{ms} + \sigma L_r i_{dr}) \quad (8)$$

Where, $V_{dr}'$and $V_{qr}'$are direct and quadrature axis rotor voltages and the equations are written as

$$V_{dr}'(K) = V_{dr}'(K-1) + K_{pdv}\{i_{der}(K) - i_{der}(K-1)\} + K_{idv}i_{der}(K) \quad (7.1)$$

$$V_{qr}'(K) = V_{qr}'(K-1) + K_{pqv}\{i_{qer}(K) - i_{qer}(K-1)\} + K_{iqv}i_{qer}(K) \quad (8.1)$$

Where,$i_{der} = i_{dr}^* - i_{dr}$, $i_{qer} = i_{qr}^* - i_{qr}$

K_{pdv} *and* K_{idv} are the gains of PI current controller, K_{pqv} *and* K_{iqv} are the gains of quadrature axis current controller.

By using dq to abc transformation, three phase reference rotor voltages are obtained from the reference rotor direct voltage (V_{dr}^*)and the reference rotor quadrature voltage (V_{qr}^*).

$$V_{ra}^* = V_{dr}^*\sin\theta_{slip} + V_{qr}^*\cos\theta_{slip} \quad (9)$$

$$V_{rb}^* = V_{dr}^*\sin(\theta_{slip} - 2\pi/3) + V_{qr}^*\cos(\theta_{slip} - 2\pi/3) \quad (10)$$

$$V_{rc}^* = V_{dr}^*\sin(\theta_{slip} + 2\pi/3) + V_{qr}^*\cos(\theta_{slip} + 2\pi/3) \quad (11)$$

6. DESIGN OF WIND TURBINE

Chopper is connected to the DC machine in wind turbine and the type of chopper used is Type-A. Torque can be obtained by using machine speed and power. Wind turbine power equation is written as

$$P_m = 0.5C_p(\lambda,\beta)\rho AV^3 \quad (12)$$

Power coefficient is a function of tip speed ratio λ and pitch angle β and is given in the equation as

$$C_p(\lambda,\beta) = C_1\left\{{}^{C_2}/_{\lambda_i} - C_3\beta - C_4\right\} exp\left({}^{C_5}/_{\lambda_i}\right) + C_6\lambda \quad (12.1)$$

7. MAXIMUM POWER POINT TRACKING

To extract maximum power MPPT algorithm is used. There are various MPPT algorithm techniques such as Incremental conductance, Perturb and observe, Fuzzy logic control, Neural network.

7.1 Grid connected photo voltaic system

The voltage that is generated from the PV panel has to be connected to the grid. A Boost converter is used to increase the voltage level. A DC-AC inverter is used in order to supply the generated DC output voltage to grid. Before connecting it to grid it has to be ensured that the output voltage of the inverter is sinusoidal and in-phase with the grid voltage. The gate pulse is generated through PWM.

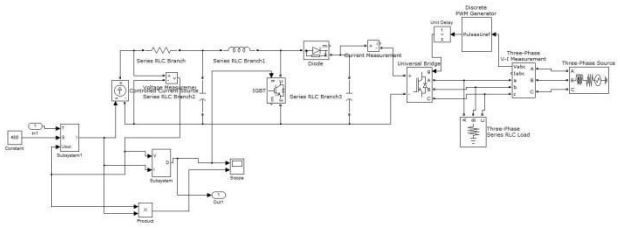

Figure-4. Grid connected PV system Simulink model.

7.2 Photovoltaic system model

The mathematical modelling of PV array is given by

$$i_{dr}^{*}(K) = i_{dr}^{*}(K-1) + K_{pd}\{\omega_{sr}(K) - \omega_{sr}(K-1)\} + K_{id}\,\omega_{sr}(K) \quad (13)$$

u_{dc} is PV array voltage

$n_p and\ n_s$ are no.of Photovoltaic cells connected in parallel and series

K is Boltzmann constant (1.38e-23, in Joules per Kelvin)

q is Electric charge (1.6e-19, in coulombs)

T is operating temperature

I_{ph} is light generated current (A)

I_{sr} is Diode saturation current (A)

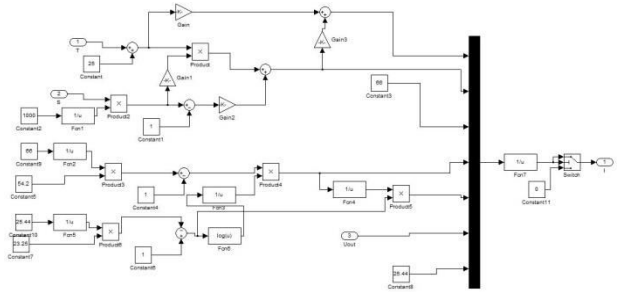

Figure-5. PV Simulink model.

The PV system equation is given as

$$C\frac{dudc}{dt} = i_{pv} - \frac{md}{2}i_d - \frac{mq}{2}i_q \quad (14.1)$$

$$L\frac{diq}{dt} = -Ri_q + Lwi_d + \frac{udc}{2}m_q - V_{sq} \quad (14.2)$$

8. SOLAR PHOTOVOLTAIC SYSTEM PROPOSED SYSTEM CONFIGURATION

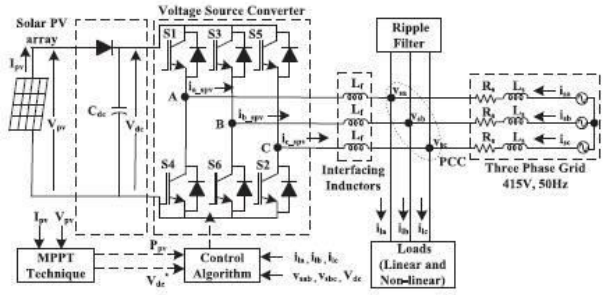

Figure-6. Schematic of SRF based system.

The proposed system has a non-linear load, VSC, MPPT technique, SRF control algorithm, SPV array system, an interfacing inductor is used to lower ripple in compensating current.

For generating gating pulses to VSC a Synchronous reference frame (SRF) algorithm is used. There are various time domain and frequency domain algorithm. Time domain algorithm such as Synchronous reference frame (SRF), PQ theory, DQ theory, Instantaneous reactive power theory. Due to high computation, sluggish and slower performance frequency domain algorithm is not preferred

9. ESTIMATION OF REFERENCE SUPPLY CURRENT

9.1 Sinusoidal-tracking algorithm

For extraction of PCC voltage of $\sin\theta_{va}$ and $\cos\theta_{va}$ components of phase 'a', phase 'b' and phase 'c' sinusoidal tracking algorithm is used. The phase 'a' voltage error (V_e) is difference between V_{sa} and V_{so}. Similarly error in phase 'b' and phase 'c' can be estimated. Lower calculation time, higher accuracy, robustness to frequency changes are the benefits of this algorithm.

Amplitude of PCC voltage is estimated by squaring all the source voltages of phase a, phase b, phase c and then sum all the three voltages, the whole is multiplied by (2/3). To the whole square-root is taken which is given in below equation as

$$V_t = \sqrt{\left({}^{2}/_{3}\right) * \left(V_{sa}^2 + V_{sb}^2 + V_{sc}^2\right)} \quad (15)$$

9.2 Estimation of phase voltage V_{pa} and V_{qa}

The in phase component of phase 'a' voltage is obtained by multiplying V_t and the $\sin\theta$component of phase 'a'

$$V_{pa} = V_t \sin\theta_{va} \quad (15.1)$$

The quadrature component of phase 'a' voltage is obtained by V_t and the $\cos\theta$component of phase 'a'

$$V_{qa} = V_t \cos\theta_{va} \quad (16)$$

Similarly, in phase and quadrature components of point of common coupling voltages of phase 'b' and phase 'c' can be estimated.

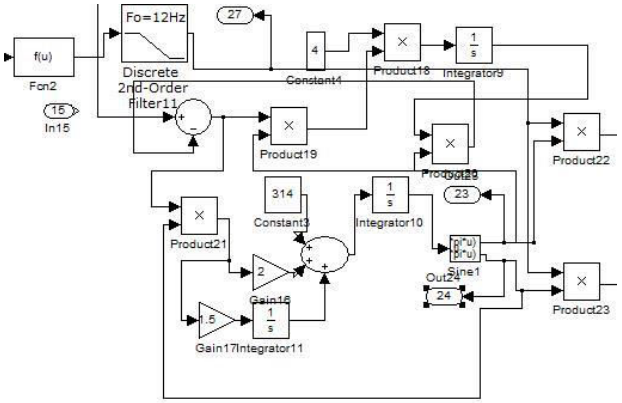

Figure-7. Simulation of phase voltage V_{pa} *and* V_{qa}.

9.3 Amplitude of load currents estimation

Real component of phase 'a' and the reactive component of phase 'a' load currents are compared with the actual load current to generate the error. The error which is obtained is then multiplied with in-phase component $(V_{pa})$and passed through a filter, whose signal is integrated with proper constant. Later the obtained signal is multiplied with (V_{pa}) in a closed loop and the real component of phase 'a' load current $(i_{lpa1})$is derived. To extract the amplitude of active power component of load current(i_{lpa}), the generated load currents root mean square is taken. The obtained signal is then transformed to peak value using gain which is shown in below Figure-8. The same is repeated for phase 'b' and phase 'c' component.

For obtaining the amplitude of reactive component of load current i_{lqa}, the above procedure is used by replacing in-phase component with quadrature component. The same is repeated for phase 'b' and phase 'c' component.

$$i_{LpA} = \frac{(i_{Lpa} + i_{Lpb} + i_{Lpc})}{3} \quad (17)$$

$$i_{LqA} = \frac{(i_{Lqa} + i_{Lqb} + i_{Lqc})}{3} \quad (18)$$

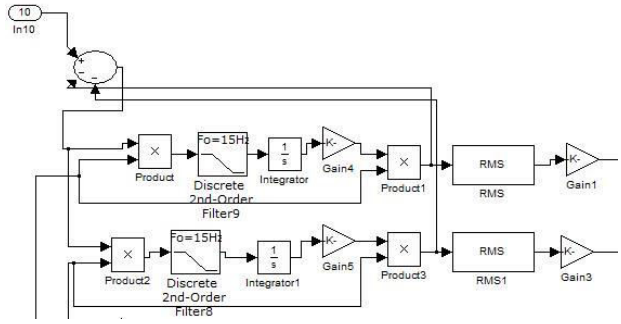

Figure-8. Phase 'a' active and reactive component of load current Simulation.

10. ESTIMATION OF THREE PHASE SENSED SUPPLY CURRENT AND GENERATION OF PULSES

The actual and the reference DC link voltages are compared and error is calculated. The obtained output is then sent to the PI controller and the signal we get is I_{Loss}. Amplitude of average fundamental active three phase load current $I_{LPA}$and the I_{Loss}current are added to get the amplitude of active component of reference supply current (I_{spt}).

$$I_{spt} = I_{LPA} + I_{Loss} \quad (19)$$

The actual and the reference terminal voltages are compared and error is calculated. The obtained output is then sent to the PI controller to maintain the PCC terminal voltage and the output we get is I_{qr}.

The I_{qr}current and amplitude of average fundamental reactive three phase load current $I_{LPA}$are subtracted to get the amplitude of reactive component of sensed supply current (I_{LPA})

$$I_{sqt} = I_{qr} - I_{LqA} \quad (20)$$

10.1 Estimation of three phase sensed supply currents

The amplitude of active component of sensed supply current (I_{sqt}) and the$\sin\theta_{va}$ component of phase 'a' are multiplied and considered as I_{sap}. The amplitude of reactive component of sensed supply current (I_{sqt}) and the $\cos\theta_{va}$component of phase 'a' are multiplied and considered as i_{saq}. Both $i_{sap}$and $i_{saq}$are added to get $i_{sa}^{*}$of phase 'a'. Similarly the sensed supply currents of phase 'b' and phase 'c' can be estimated.

$$i_{sa}^{*} = i_{sap} + i_{saq} \quad (21)$$

$$i_{sb}^{*} = i_{\boldsymbol{sbp}} + i_{sbq} \quad (22)$$

$$i_{sc}^{*} = i_{scp} + i_{scq} \quad (23)$$

where,

$$i_{sap} = I_{spt} \sin\theta_{va} \; ; i_{saq} = I_{sqt} \cos\theta_{va} \quad (21.1)$$

$$i_{sbp} = I_{spt} \sin\theta_{vb} \; ; i_{sbq} = I_{sqt} \cos\theta_{vb} \quad (22.1)$$

$$i_{scp} = I_{spt} \sin\theta_{vc} \; ; i_{scq} = I_{sqt} \cos\theta_{vc} \quad (23.1)$$

The actual supply current $(i_{sap}, i_{sbp}, i_{scp})$and the sensed supply current $(i_{sa}^*, i_{sb}^*, i_{sc}^*)$ are compared using relational operator and by the logical operator to generate the gating pulse for the IGBT of voltage source converter (VSC).

11. CALCULATION OF DC-LINK VOLTAGE (V_{dc})

$$V_{dc} = \frac{2\sqrt{2}*V_{LL}}{\sqrt{3}*m} \quad (24)$$

Where $V_{LL}$is ac line output voltage and m is the modulation index and is taken as 1.

12. CALCULATION OF INTERFACING INDUCTOR

$$L_f = \frac{(\sqrt{3}*m*V_{dc})}{(12*k*f_{sw}*I_{cr})} \quad (25)$$

f_{sw} is the switching frequency,V_{dc} is the DC-link voltage, $I_{cr}$is the percentage range of ripple current.

13. CALCULATION OF DC-LINK CAPACITOR

$$C_{dc} = \frac{6\propto\left\{V_{ph}(\mu I_c)t\right\}}{(V_{dc}^2 - V_{dc1}^2)} \quad (26)$$

Where V_{ph} is the supply phase voltage, $I_c$is the phase current, t is recovered DC-link voltage time, $V_{dc}$is nominal DC link voltage, Overloading factor is α.

14. PERTURB AND OBSERVE ALGORITHM

MPPT algorithm is used to extract maximum power. Perturb and observe method is an MPPT technique used to enhance efficiency of the solar energy conversion of PV system. The calculation of PV output power is based on MPPT algorithm. The voltage and current variables are assigned first, secondly the power$(P(K))$is determined. The obtained output power $(P(K))$is compared with the $(P(K-1))$and adds a perturbation to the output voltage. Later it compares the present power with the actual power. Depend on increase or decrease of power the use of disturbance changes. When power is increased, the actual disturbance is used. Similarly with decrease in power the disturbance is changed. Hence perturb and observe algorithm disturbs the voltage to get the maximum power. The process is repeated until we get the maximum power and also the choppers duty cycle is varied.

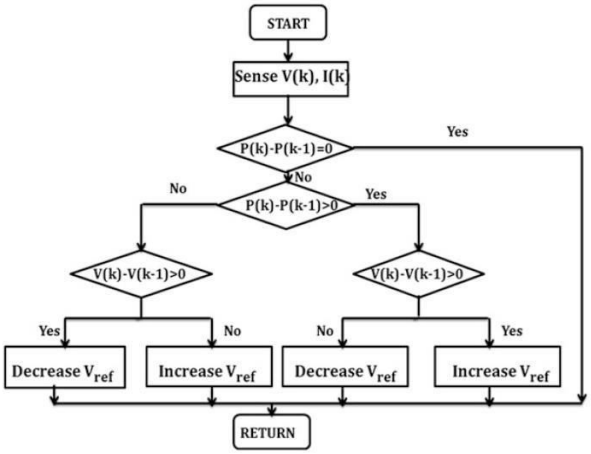

Figure-9. Perturb and observe algorithm.

By using the above P & O algorithm procedure the Simulink model has been designed and simulated in MATLAB.

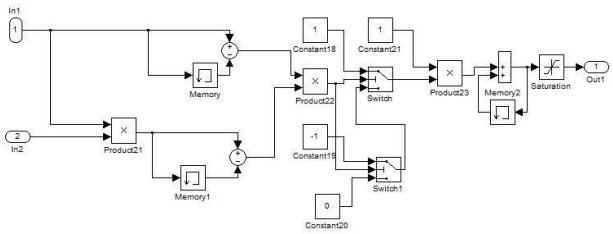

Figure-10. Perturb and observe Simulink model.

14.1 SPV array model and simulation

The solar system model consists of a required number of SPV cells normally mentioned as PV modules, connected in series or in parallel to attain the required voltage output.

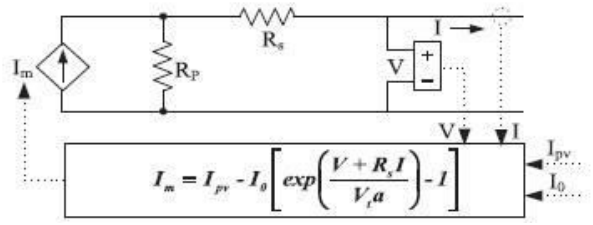

Calculation of I_m

$$I_m = I_{pv} - I_o \left[\exp\left(q * \frac{(V+R_S I)}{KT\alpha}\right)\right] \quad (27)$$

Where

I_{pv} = SPV current
I_o = Short circuit current
q = Electron charge (1.60217646e-19)
K = Boltzmann constant (1.3806503e-23)
α = Diode constant (1.3)

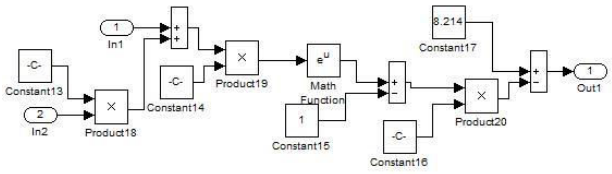

Figure-11. Simulink model of PV equation.

15. SELECTION OF INTERFACING INDUCTOR

The interfacing inductor is placed between the grid side converter and the point of common coupling. The design is based on the GSC current, DC-link voltage and the switching frequency of the GSC. The inductor value is calculated using the equation

$$L_i = \frac{\sqrt{3mV_{dc}}}{12af_m\Delta i_{gc}} \quad (28)$$

16. SELECTION OF DC-LINK VOLTAGE

For obtaining the DC-link voltage, rotor voltage and PCC voltage are mainly required. The selection is done by considering from rotor side and from GSC side. The design is selected by considering only the PCC voltage. The calculation of DC link voltage is given as

$$V_{dc} \geq \frac{2\sqrt{2}}{\sqrt{3m}}V_{ab} \quad (29)$$

17. MATLAB SCHEMATICS OF DFIG FOR WECS WITH INTEGRATED ACTIVE FILTER CAPABILITIES

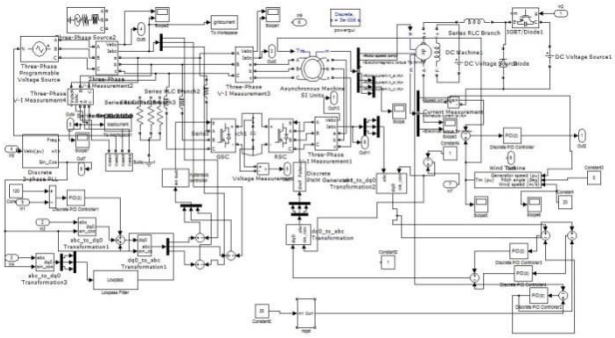

Figure-12. DFIG for WECS with integrated active filter capabilities Simulink model.

The DFIG systemis designed and the circuit has been simulated in MATLAB. Two subsystems are created fot the hysteresis controller and for the MPPT technique.

To estimate the wind speed turbine output power and the shaft speed are required in case of back-to-back connected converter. With the estimated speed the generator output and the shaft speed is obtained. DFIG along with induction generator are excellent for high power applications.

17.1 Waveform of grid voltage and current

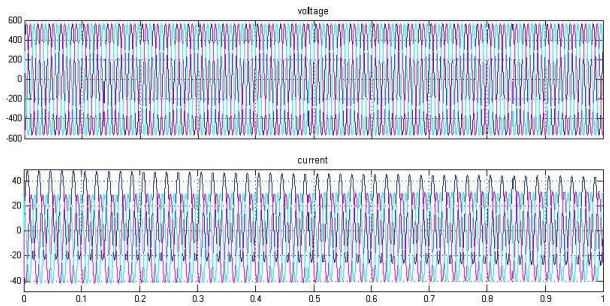

Figure-13. Grid voltage and current simulated waveform.

17.2 Waveform ofload current

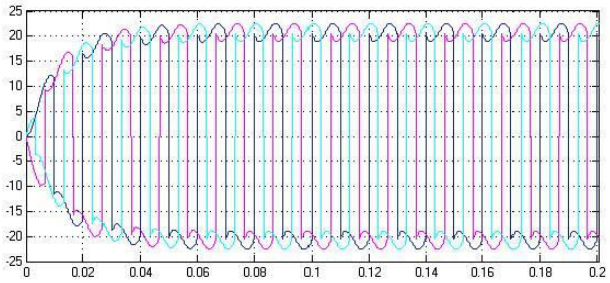

Figure-14. Simulated waveform of load current.

17.3 Waveform ofload voltage

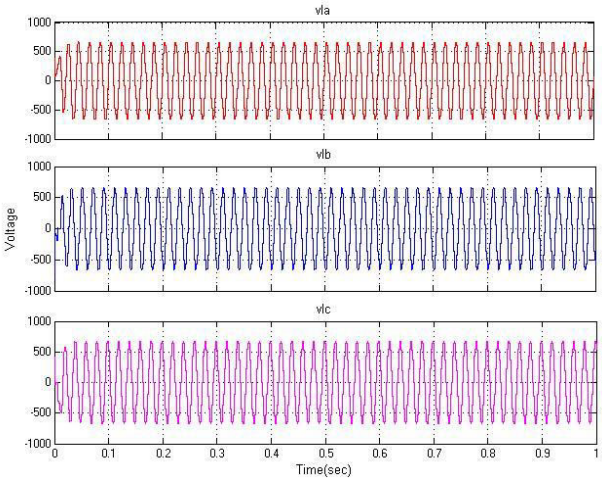

Figure-15. Simulated waveform of load voltage.

17.4 %THD of source current

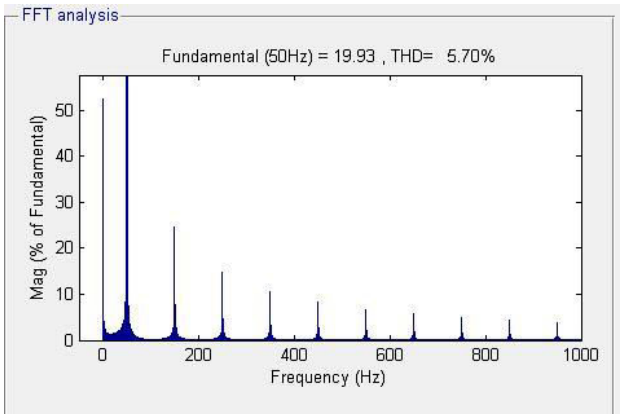

Figure-16. Source current harmonic spectrum is shown above and the %THD is value is 5.70%.

17.5 %THD of load current

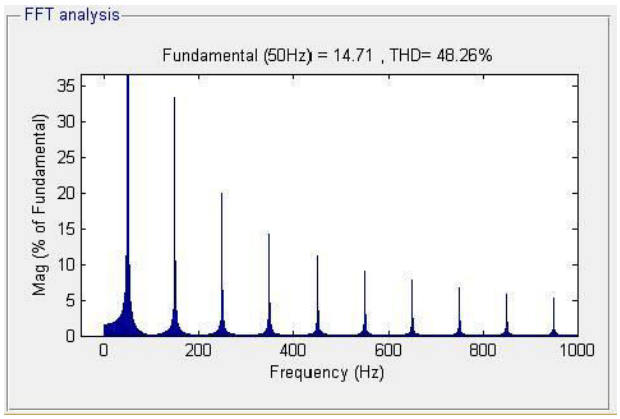

Figure-17. Load current harmonic spectrum is shown above and the %THD is 48.26%.

18. MATLAB SCHEMATICS OF SRF-BASED CONTROL ALGORITHM FOR SINGLE STAGE THREE-PHASE GRID INTEGRATED SOLAR PV SYSTEM

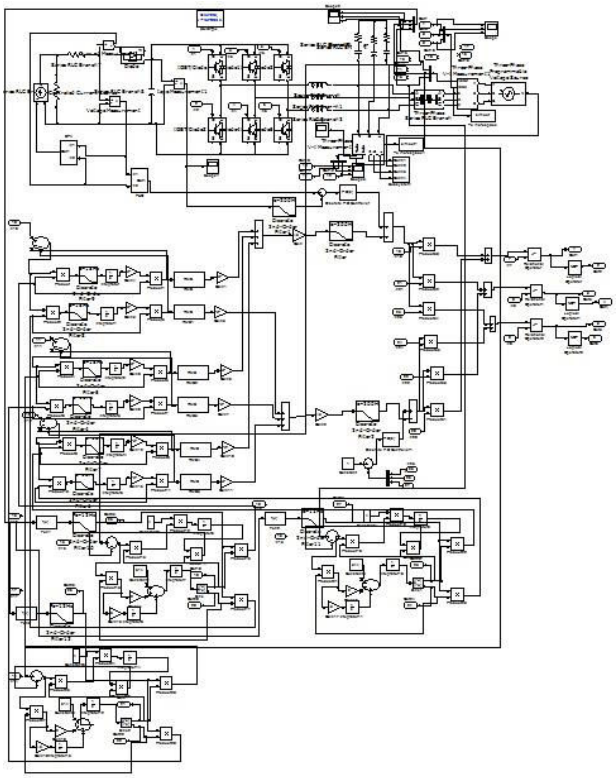

Figure-18. SRF-based control algorithm for single stage three-phase grid integrated solar PV system Simulink model.

18.1 Waveform of source current

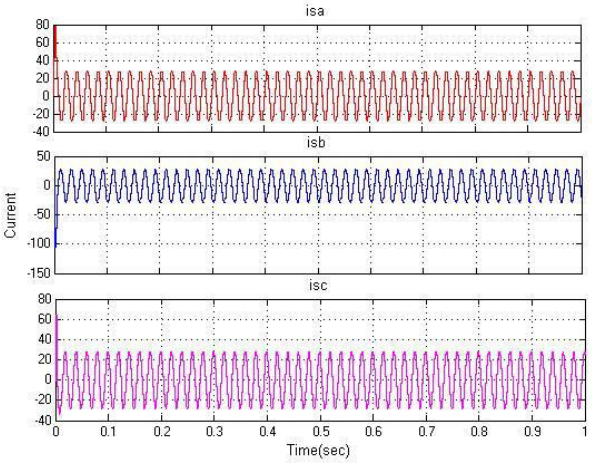

Figure-19. Source current simulated waveform.

18.2 Waveform of load current

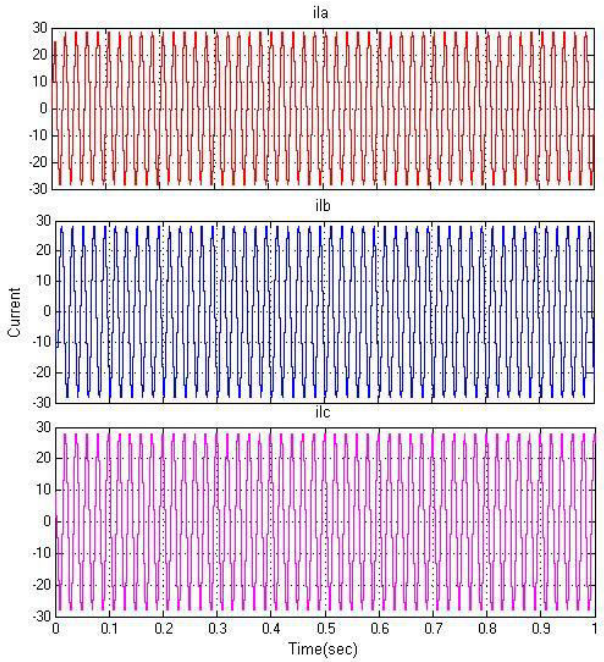

Figure-20. Load current simulated waveform.

18.3 Waveform OFDC-link voltage

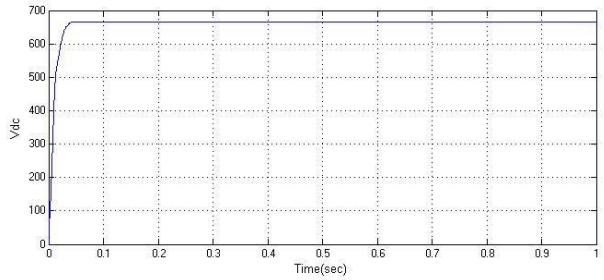

Figure-21. DC-link voltage simulated waveform.

18.4 Waveform ofsource voltage

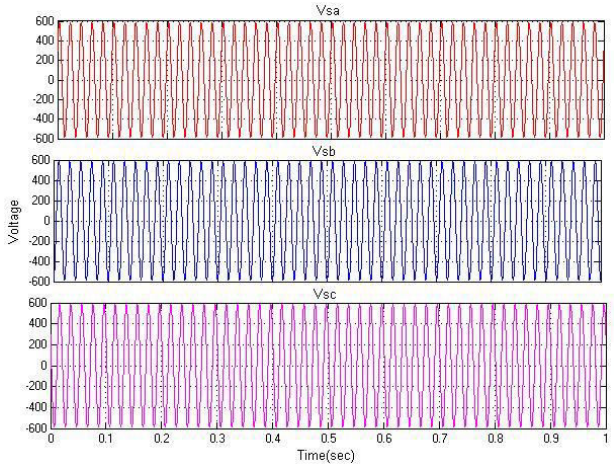

Figure-22. Source voltage simulated waveform.

18.5 Waveform of load voltage

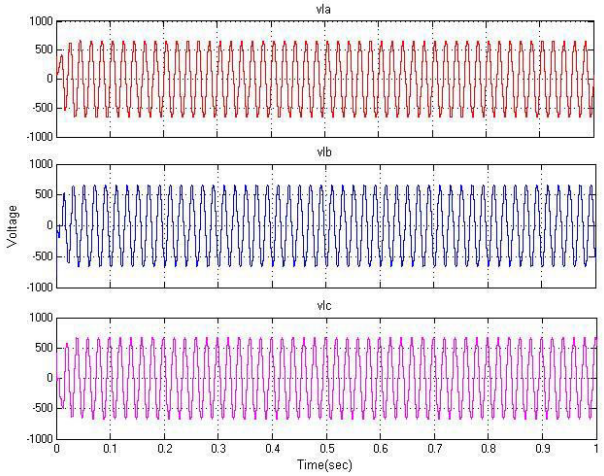

Figure-23. Load voltage simulated waveform.

18.6 THD% of source current

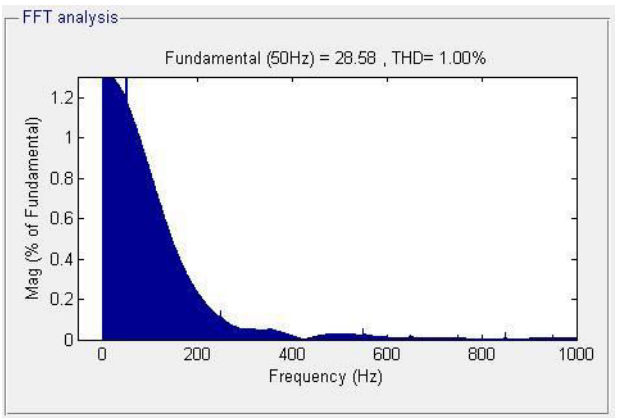

Figure-24. The harmonic spectrum of source current is shown above and the %THD is value is 1.00%.

From Figure-24 it is inferred that the %THD of source current is below 5% according to the IEEE-519 standard.

Table-2. Comparison between WECS and SPV system.

WECS	SPV System
Source %THD is 5.70%	Source %THD is 1%

From Table-2 it is inferred that the %THD of source current in SPV system is below 5% and is in accordance with the IEEE-519 standard. Hence from the Table-2 it can be said that the SPV system is best when compared with WECS system in maintaining IEEE standard and is effective in improving power quality problems.

19. CONCLUSIONS

The basic operation of DFIG and its control using AC/DC/AC converter is performed and discussed. DFIG

system is used to get better efficiency and control which is connected to the grid side. Grid side converter (GSC) is used to maintain DC-link voltage constant whereas Rotor side converter (RSC) is used to provide active and reactive power control. In case of second system, the control algorithm is based on SRF adaptive filtering technique. Grid integrated SPV system is designed based on this technique. Simulation has been done and the values are tabulated. Maximum power has been extracted by using MPPT technique. The entire system has been designed, simulated in MATLAB and the obtained results are verified. From the obtained results it is inferred that the Solar systems source % THD is below 5% that is within limit and the load % THD is above 5%. Hence solar system is more effective in improving power quality problems and mitigating harmonics than WECS. Single stage SPV system is more effective in reducing losses than conventional double stage.

APPENDIX

DFIG: 3.7kw, R_s = 1.32ohm, L_{ls}= 6.832mH, R_2 = 1.708ohm,L_{lr} = 6.832mH, R_c = 419.64ohm, L_m= 0.219H, J=0.1878kg.m^2, stator to rotor turns ratio N_r/N_s =1/2.

DC Machine: R_a=2.5 ohms, R_f=280.3 ohms, L_a=4.8mH, L_f=5.2mH.

Controller gains-Speed controller: K_{pd} =0.25, K_{id}=0.3, Current controller: K_{pdv} =100, K_{pqv} =100, K_{idv} =130, K_{iqv} =130, DC-link voltage controller: K_{pdc} =1.5, K_{idc}=1

SPV System: SPV voltage V_{MPP}= 26.3 V; SPV module current I_{MPP}= 7.61 A, DC PI Controller: K_{pd} = 0.9, K_{id}= 0.75, AC PI Controller: K_{pt}= 0.91, K_{it} = 0.7, Ripple Filter: R_f= 4W, C_f = 5μF, Interfacing Inductor: L_f= 2.5mH, Non-linear load: R =15W, L = 50mH.

REFERENCES

[1] N. K. Swami Naidu and Bhim Singh. 2015. Doubly Fed Induction Generator for Wind Energy Conversion systems With Integrated Active Filter Capabilities. IEEE Transactions on Industrial Informatics. 11(4): 923-933.

[2] G. Todeschini and A. E. Emanuel. 2010. Wind Energy Conversion system as an Active Filter: Design and Comparison of Three Control Systems. IET. Renew. Power Gener. 4(4): 341-353.

[3] N. Krishna Swami Naidu, Bhim Singh. 2014. Sensorless Control of Single Voltage Source Converter Based Doubly Fed Induction Generator for Variable Speed Wind Energy Conversion System. IET Power Electronics. 7: 2996-3006.

[4] Saiful Islam Rasel, Rahanuma Nireen Ali, Md. Sarwar Uddin Chowdhury. 2015. Design and Simulation of Grid Connected Photot Voltaic System Using Simulink. International Conference on Advances in Electrical Engineering. 238-242.

[5] B. Singh and J. Solanki. 2009. An implementation of an adaptive control algorithm for a three-phase shunt active filter. IEEE Trans. Ind. Electron. 56(8): 2811-2820.

[6] Rahul Kumar Agarwal, Ikhlaq Hussain and Bhim Singh. 2016. LMF-Based Control Algorithm for Single Stage Three-Phase Grid Integrated Solar PV System. IEEE Transactions on Sustainable Energy. 7(4): 1379-1387.

[7] I. Hussain and B. Singh. 2014. Grid integration of single stage solar PV power generating system using 12-pulse VSC. in Proc. IEEE 6th India Int. Conf. Power Electron. 10(8): 1-6.

[8] Ahmed M. Atallah, Almoataz Y. Abdelaziz and Raihan S. Jumaah. 2014. Implementation of Perturb and Observe MPPT of PV System with Direct Control Method Using Buck and Buck-boost Converters. Emerging Trends in Electrical, Electronics & Instrumentation Engineering: An International Journal (EEIEJ. 1(1).